

Strong correlation effects in the fullerene C₂₀ studied using a one-band Hubbard model

Fei Lin,¹ Erik S. Sørensen,² Catherine Kallin,² and A. John Berlinsky²

¹*Department of Physics, University of Illinois at Urbana-Champaign, Urbana, Illinois 61801, USA*

²*Department of Physics and Astronomy, McMaster University, Hamilton, Ontario, Canada L8S 4M1*

(Received 8 April 2007; published 25 July 2007)

The smallest fullerene, dodecahedral C₂₀, is studied using a one-band Hubbard model parametrized by U/t . Results are obtained using exact diagonalization of matrices with linear dimensions as large as 5.7×10^9 , supplemented by quantum Monte Carlo. We report the magnetic and spectral properties of C₂₀ as a function of U/t and investigate electronic pair binding. Solid forms of C₂₀ are studied using cluster perturbation theory, and evidence is found for a metal-insulator transition at $U \sim 4t$. We also investigate the relevance of strong correlations to the Jahn-Teller effect in C₂₀.

DOI: [10.1103/PhysRevB.76.033414](https://doi.org/10.1103/PhysRevB.76.033414)

PACS number(s): 71.10.Li, 71.20.Tx, 71.30.+h

The smallest fullerene, C₂₀, contains 12 carbon pentagons (and no hexagons) forming a dodecahedron in a perfect representation of a platonic solid. Among the many possible isomers of C₂₀, it is not obvious that this dodecahedral fullerene cage should be the most stable, and theoretical studies^{1,2} have reached different conclusions. In addition, unlike C₆₀, dodecahedral C₂₀ is not spontaneously formed in condensation or cluster annealing processes,³ and its extreme curvature and strong reactivity led to doubts about its stability. It therefore created considerable excitement when Prinzbach *et al.*⁴ succeeded in producing the dodecahedral fullerene isomer of C₂₀ in the gas phase. Experiments have also shown evidence for solid phases of C₂₀,^{5,6} although the crystal structure is still debated. Density-functional studies of the solid forms of C₂₀ (Refs. 6–10) have suggested different crystal structures with the most promising candidate, C₂₀ cages connected by C atoms to form a 22 atom unit cell,^{6,9} predicted to become superconducting upon doping with Na.⁹ A simple-cubic-like phase of C₂₀ has also been speculated to become superconducting.⁸ In their proposal for a purely electronic mechanism for superconductivity in C₆₀, Chakravarty *et al.*¹¹ have stressed the importance of structure at the mesoscale.¹² Along with the molecular solids formed by C₆₀, solid phases of C₂₀ would be ideal candidates for this picture, and a detailed understanding of these phases would be of great interest. Strong correlation effects are likely to be important in C₂₀, and previous studies^{1,2,6,7,9,10,13} have treated these correlation effects approximately. Here, we show that within a Hubbard model description, an almost exact treatment is possible using a large-scale numerical approach.

Our starting point is the one-band Hubbard Hamiltonian on a single C₂₀ molecule defined as:

$$H = -t \sum_{\langle ij \rangle \sigma} (c_{i\sigma}^\dagger c_{j\sigma} + \text{H.c.}) + U \sum_i n_{i\uparrow} n_{i\downarrow}, \quad (1)$$

where $c_{i\sigma}^\dagger$ ($c_{i\sigma}$) is an electron creation (annihilation) operator, U is the on-site Coulomb interaction, and $n_{i\sigma}$ is the number of electrons on site i with spin σ . Due to the extreme curvature of C₂₀, we expect t to be smaller than typical values for C₆₀ while U should remain close to that of C₆₀. Consequently, we expect that a realistic value for U/t valid for C₂₀ is likely *larger* than the value of $U/t \sim 4$ (Ref. 14) used for

C₆₀, implying that strong correlation effects play a more crucial role in the physics of C₂₀. The Hamiltonian, Eq. (1), is a simplified model of C₂₀ and our use of this model is motivated by two distinct rationales. First, this model is of central importance in the theory of strongly correlated electronic systems. The C₂₀ structure allows us to study strong correlation effects in a relatively large system using *exact* numerical methods. Second, from earlier work on C₆₀ molecules, we have found that many features, such as the dependence of extended x-ray-absorption fine structure spectra on molecular orientation, are equally well modeled by detailed local-density approximation (LDA)-type calculations¹⁵ as by quantum Monte Carlo (QMC) simulations of the Hubbard model.¹⁴ On the other hand, it is well established that the Hubbard model provides a more realistic treatment of systems close to a metal-insulator transition. The magnetic metal to nonmagnetic insulator transition that we find for increasing U (see below) would be difficult to model in LDA.

Even though C₆₀ and C₂₀ share the same symmetry group, I_h , noninteracting C₂₀ is a metal while neutral C₆₀ is an insulator. This is evident from the Hückel molecular orbitals (HMOs) shown in Fig. 1(a). The highest occupied molecular orbital G_u is fourfold degenerate, containing two electrons for the neutral molecule. The lowest unoccupied molecular orbital G_g is considerably higher in energy. Here, we shall mainly be concerned with neutral, one- and two-electron doped molecules which only involves the G_u levels.

Due to the orbital degeneracy of the neutral C₂₀ molecule, the Jahn-Teller effect is expected to be important. The electronic G_u levels can couple to the A_g , G_g , and H_g Jahn-Teller phonon modes. We focus exclusively on the effects of a static distortion. The inclusion of dynamic phonons in our model would be highly interesting but is not possible within our exact diagonalization approach. Theoretical studies have argued for the resulting lowered symmetry to be C_2 ,¹⁶ D_{5d} ,¹⁷ C_{2h} ,¹⁸ C_i ,¹⁹ and D_{3d} .^{2,20} Here, we follow Yamamoto *et al.*²⁰ and assume a static deformation of D_{3d} symmetry. The bond lengths for the optimal D_{3d} structure are²⁰ $a_{ab} = 1.464 \text{ \AA}$, $a_{bc} = 1.469 \text{ \AA}$, $a_{cc'} = 1.519 \text{ \AA}$, and $a_{cc''} = 1.435 \text{ \AA}$. (See Fig. 1 of Ref. 20.) We parametrize the distortion by letting t_a , the hopping along the bond of length a , depend on a parameter ϵ in the following way: $t_a/t = 1 - \epsilon(a - \bar{a})/\bar{a}$. Here, \bar{a}

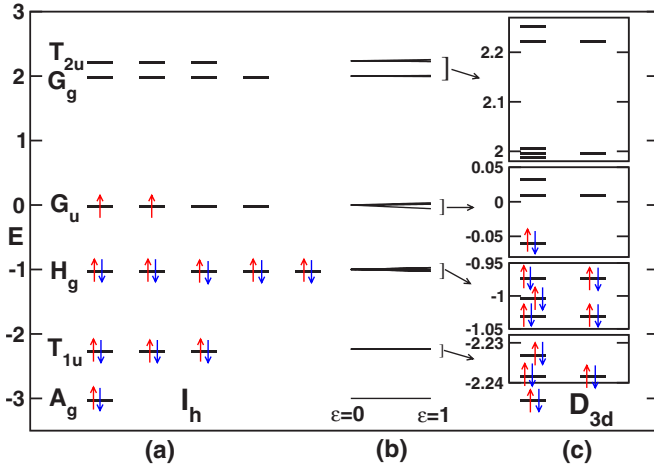


FIG. 1. (Color online) (a) HMO levels for neutral C₂₀ with I_h symmetry. (b) The Walsh diagram showing the evolution of the levels with the distortion ϵ toward D_{3d} symmetry. (c) HMO levels for the molecule with D_{3d} symmetry ($\epsilon=1$).

$=1.4712 \text{ \AA}$ is the average over C₂₀ of the above bond lengths. Then, $\epsilon=0$ and 1 correspond to the I_h and D_{3d} structures, respectively. At $\epsilon=1$, the maximal deviation of t_a/t from 1 is less than 3.5%. In Fig. 1, the Walsh diagram for the evolution of the I_h levels with the distortion ϵ is shown along with the HMO levels for the optimal D_{3d} structure for $\epsilon=1$.

Numerics. Our exact diagonalization (ED) work is performed in a completely parallel fashion using SHARCNET facilities. In addition to the total particle number and total S_z components of the spin, we also exploit the S₁₀ (S₆) subgroup symmetry present in the I_h (D_{3d}) symmetry group. The basic element of this subgroup is a rotation of $2\pi/10$ ($2\pi/6$) around the face of a pentagon (around a vertex) combined with reflection. We denote the corresponding pseudoangular momenta by j_{10} (j_6). After symmetry reductions, the size of the Hilbert space at half filling for the singlet states of the neutral molecule is 3 418 725 024 for the I_h configuration and 5 699 353 088 for the D_{3d} distorted configuration. The Hamiltonian is applied to vectors distributed across P processors and each processor communicates with all others using nonblocking communications and a carefully designed buffering strategy. The design is efficient enough that the

time of each Lanczos step is dominated by computation rather than communication and scales nearly linearly with P . For $P=64$, a Lanczos iteration for the I_h (D_{3d}) configuration is completed in 540 (980) s.²¹ Dynamical properties are calculated using standard ED techniques.²² Our quantum Monte Carlo (QMC) follows standard methods²³ with ground-state energies obtained from projector QMC, while spectral functions are obtained from finite temperature, $\beta=10/t$, QMC²³ combined with maximum entropy methods.²⁴

Magnetic properties. From the noninteracting HMO levels in Fig. 1, it would appear that the ground state of the neutral molecule is magnetic at small U/t . Our ED and QMC work confirms that this is the case for the I_h configuration for $U/t \leq 3$, where the ground state is observed to be an orbitally degenerate triplet, $S=1$, occurring at $j_{10}=0, \pm 2$. Table I gives the few lowest energy levels, labeled by spin and pseudoangular momentum, for the cases of $U/t=2$ and 5. For $U/t=5$, we find that the ground state for the I_h configuration is a nondegenerate singlet, $S=0$, occurring at $j_{10}=5$, and separated from the lowest-lying excitation, another singlet at $j_{10}=0, \pm 2, \pm 4$, by a gap of $0.1t$. The lowest triplet excitation is found at $j_{10}=0, \pm 2$. This ordering of levels continues to hold for larger U/t , although the energy scale decreases with increasing U . The degeneracies and excitation gaps at large U/t agree with ED studies of the dodecahedral $S=1/2$ antiferromagnetic Heisenberg model.²⁵ In fact, the ground-state energy calculated for neutral C₂₀ in the large U limit ($U > 50$) can be related to the ED result for the Heisenberg model to the accuracy that the latter has been calculated.²⁶ From Table I, it is clear that the system crosses over from a triplet to singlet ground state between $U/t=2$ and $U/t=5$. Assuming a linear dependence on U/t of the energy of the triplet states at $j_{10}=0, \pm 2$ and the singlet at $j_{10}=5$, we estimate that this transition occurs at $U_c/t \sim 4.10$, indicated by the solid vertical line in Fig. 2. The fact that the ground state for the neutral molecule for $U > U_c$ is a nondegenerate singlet implies that the molecule is stable against Jahn-Teller distortions for large U .

Surprisingly, the D_{3d} distorted molecule follows the same pattern with the exception that at $U/t=0$, the unique ground state is a singlet. However, once U/t becomes of order of the splitting of the G_u levels, $\sim 0.0686t$, the ground state becomes a triplet. At $U/t=0.5$ and 2, we find that this ground state triplet occurs at $j_6=0$ with a number of low-lying triplet

TABLE I. Lowest energy levels (in units of t) of the neutral C₂₀ molecule for $U=2t, 5t$, labeled by spin and pseudoangular momentum, for the I_h ($j=j_{10}$) and D_{3d} ($j=j_6$) configurations.

| | $U=2t$ | S | j | $U=5t$ | S | j |
|-----------------|----------------|-----|-----------|----------------|-----|-----------|
| I _h | -20.5983834340 | 1 | 0, ±2 | -12.1112842959 | 0 | 5 |
| | -20.5981592741 | 1 | 0, ±4 | -12.0123014488 | 0 | 0, ±2, ±4 |
| | -20.5920234655 | 0 | 0, ±2, ±4 | -11.8770332831 | 1 | 0, ±2 |
| | -20.0527029539 | 0 | 5 | -11.8472120431 | 1 | ±1, ±3 |
| D _{3d} | -20.6757641960 | 1 | 0 | -12.1204684092 | 0 | 3 |
| | -20.6462557924 | 1 | ±2 | -12.0921677742 | 0 | 0 |
| | -20.6166968560 | 0 | ±2 | -11.9197052918 | 1 | 3 |
| | -20.0754248172 | 0 | 3 | -11.8974914914 | 1 | 0 |

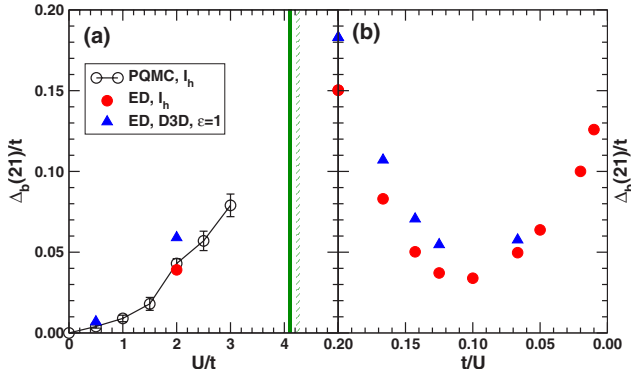


FIG. 2. (Color online) Electronic pair binding energy $\Delta_b(21)/t$ as a function of U/t . ED (●) and QMC (○) results for the molecule with I_h symmetry. ED results (▲) for the molecule with D_{3d} ($\varepsilon=1$) symmetry. The solid (crossed) vertical line indicates U_c/t for neutral I_h (D_{3d}) molecules. (a) Δ_b versus U/t for $U/t \leq 5$. (b) Δ_b versus t/U for $5 \leq U/t \leq 100$.

states above it. The Jahn-Teller distortion has therefore completely removed the orbital degeneracy leaving only a Kramer's degeneracy. At $U/t=2$, the lowest-lying excitation is a triplet at $j_6=\pm 2$, and the lowest-lying singlet, with a gap approximately twice as large, is at the same $j_6=\pm 2$. As for the I_h configuration, we observe that the ground state is a singlet at $U/t=5$ occurring at $j_6=3$. An analysis similar to the I_h case yields $U_c/t \sim 4.19$, indicated by the crossed vertical line in Fig. 2, very close to the estimate for the I_h configuration. Again, the system remains in a singlet state for larger values of U/t .

Pair binding. The purely electronic mechanism for superconductivity^{11,12} is based on a favorable pair binding energy. The pair binding energy is defined as the energy difference between having two extra electrons on the same and on separate molecules:

$$\Delta_b(N+1) = E(N+2) - 2E(N+1) + E(N). \quad (2)$$

When negative, it is favorable to have the two electrons on the same molecule providing a purely electronic mechanism

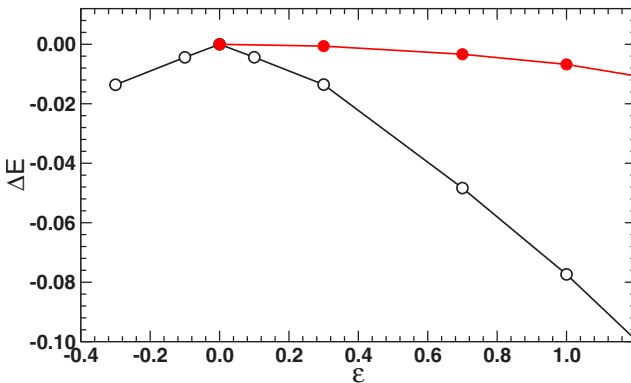


FIG. 3. (Color online) Shift in the ground-state energy of the neutral molecule, ΔE , versus the distortion ε . The Jahn-Teller instability is quite pronounced for $U/t=2$ (○), but it is essentially absent for $U/t=8$ (●).

for superconductivity. Intriguingly, for neutral C_{12} ,²⁷ as well as for several related models,¹² it is known that Δ_b is negative. For C_{60} , perturbative results indicated that the observed superconducting phase has its origins in a negative Δ_b .^{11,28,29} However, earlier QMC results³⁰ find no binding, suggesting that either low order perturbation theory is inadequate or that the QMC results are not sufficiently accurate to measure the binding. Thus, it is of considerable interest to obtain exact results for C_{20} which can then be used to test the accuracy of QMC.

Our results for $\Delta_b(21)/t$ are shown in Fig. 2. We first consider results for the I_h configuration of C_{20} . The QMC results (○) and the ED results (●) are in excellent agreement, and for $U/t \leq 3$, they show that Δ_b is positive and pair binding is *suppressed*. (For $U > U_c$, it is not possible to perform QMC calculations due to the sign problem.) The ground state for the neutral molecule is now a singlet and our ED results again clearly indicate that pair binding is *not* favored. As U/t increases, Δ_b reaches a minimum at $U/t \sim 10$. Then, as $U/t \rightarrow \infty$, Δ_b approaches a finite positive value, consistent with the exact result showing the absence of pair binding for electron doping in the $U=\infty$ limit.³¹

We can only calculate the pair binding for the Jahn-Teller distorted molecule in an approximate manner since the distortion will depend on the electron doping. We make the simplifying assumption that the distortion is static, of D_{3d} symmetry, and independent of doping. We find that the Jahn-Teller distortion makes pair binding less favorable. We have also investigated the effects of nearest neighbor repulsion V in an extended Hubbard model and find that it too works against pair binding.²¹ An important difference between the ground states for small and large U is the relative stability of the gapped state for $U > U_c$ against the Jahn-Teller distortion. In Fig. 3, we show results for the shift in the ground-state energy versus ε where the strong dependence on ε for $U/t=2$ is indicative of the molecule being Jahn-Teller active. By

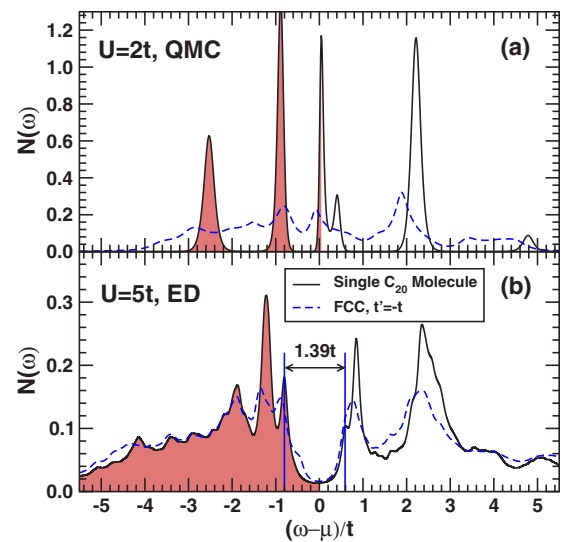


FIG. 4. (Color online) Density of states $N(\omega)$ at (a) $U=2t$ from QMC and at (b) $U=5t$ from ED. In both panels, the density of states for the C_{22} fcc lattice obtained from CPT with $t'=-t$ is shown as a dashed line.

contrast, for $U/t=8$, the dependence on ε is very shallow, signaling that the I_h structure is stable.

Spectral functions and solid C_{20} . Next we calculate the density of states $N(\omega)$ and wave-vector dependent spectral functions $A(k, \omega) = -(1/\pi)\text{Im}[G(k, \omega + E_0 + i\eta)]$ for a three-dimensional solid of C_{20} molecules. Here, E_0 is the ground-state energy and G the single-particle Green's function. The calculation is performed by cluster perturbation theory^{32,33} (CPT) using QMC and ED data. In all cases, delta functions were treated as Lorentzians with a broadening of $\eta=0.1$. The QMC version of this method was applied earlier to the case of C_{60} monolayers.¹⁴ We idealize the hypothetical fcc C_{22} structure^{6,9} by a model in which the bridging C atoms are replaced by effective hopping integrals, $t' = -t$, between C_{20} molecules. The resulting $N(\omega)$ and $A(k, \omega)$ are shown in Figs. 4 and 5 for $U/t=2$ and 5. Also shown in Fig. 4 are the single-molecule densities of states. For $U/t=2$, which lies in the middle of the region of triplet ground state, the solid of undistorted I_h molecules is metallic with a complicated Fermi surface, while, for $U/t=5$, in the region of singlet ground state, the solid is insulating with a gap of about $1.4t$ and some narrowing of the "bands" close the Fermi energy is observed.

In conclusion, we have calculated the ground-state properties and spectral functions of the Hubbard model on a C_{20} molecule using ED and QMC and have shown that pair binding is not favored in this molecule. We have identified a ground-state crossing at $U_c \sim 4.1t$ where the system switches from a triplet state which is unstable against a Jahn-Teller distortion to a gapped singlet state which is stable. Extending this result using CPT, we identify a metal-insulator transition for the bulk solid at $U = U_c$. If the symmetric, I_h , form of C_{20}

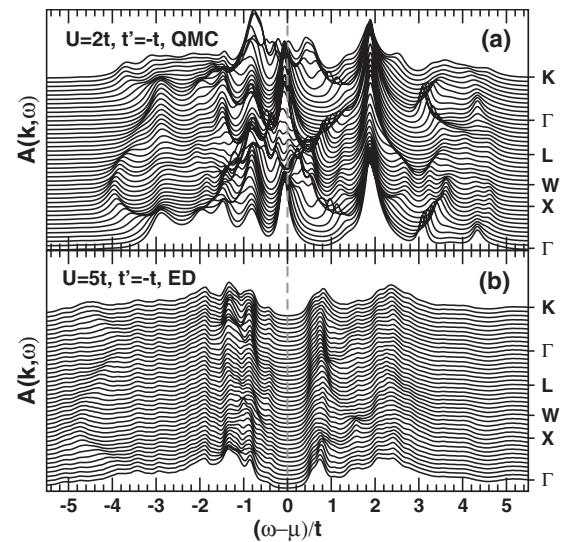


FIG. 5. Spectral functions with the chemical potential μ determined from $N(\omega)$ in Fig. 4. Results for the C_{22} fcc lattice with (a) $U=2t$ and (b) $U=5t$ as obtained from CPT with $t' = -t$. The k -axis labels refer to standard notation for the FCC Brillouin zone.

is found to be stable, a possible explanation would be that it is stabilized by correlations resulting from $U > U_c$.

This project was supported by the NSERC, CIAR and CFI. F.L. is supported by the US Department of Energy under Award No. DE-FG52-06NA26170. A.J.B. and C.K. gratefully acknowledge the hospitality and support of the Stanford Institute for Theoretical Physics, where part of this work was carried out. All the calculations were carried out at SHARCNET supercomputing facilities.

- ¹M. Sawtarie *et al.*, Phys. Rev. B **49**, 7739 (1994); J. C. Grossman *et al.*, Phys. Rev. Lett. **75**, 3870 (1995); P. R. Taylor *et al.*, Chem. Phys. Lett. **235**, 558 (1995); R. O. Jones and G. Seifert, Phys. Rev. Lett. **79**, 443 (1997).
- ²G. Galliet *et al.*, Phys. Rev. B **57**, 1860 (1998).
- ³H. W. Kroto, Nature (London) **329**, 529 (1987).
- ⁴H. Prinzbach *et al.*, Nature (London) **407**, 60 (2000).
- ⁵Z. Wang *et al.*, Phys. Lett. A **280**, 351 (2001).
- ⁶Z. Iqbal *et al.*, Eur. Phys. J. B **31**, 509 (2003).
- ⁷M. Côté *et al.*, Phys. Rev. B **58**, 664 (1998); S. Okada *et al.*, *ibid.* **64**, 245405 (2001).
- ⁸Y. Miyamoto and M. Saito, Phys. Rev. B **63**, 161401(R) (2001).
- ⁹I. Spagnolatti *et al.*, Europhys. Lett. **59**, 572 (2002).
- ¹⁰Z. Chen *et al.*, Chem.-Eur. J. **10**, 963 (2004).
- ¹¹S. Chakravarty *et al.*, Science **254**, 970 (1991).
- ¹²S. Chakravarty and S. A. Kivelson, Phys. Rev. B **64**, 064511 (2001).
- ¹³R. López-Sandoval and G. M. Pastor, Eur. Phys. J. D **38**, 507 (2006).
- ¹⁴F. Lin *et al.*, Phys. Rev. B **75**, 075112 (2007).
- ¹⁵W. L. Yang *et al.*, Science **300**, 303 (2003).
- ¹⁶B. L. Zhang *et al.*, J. Chem. Phys. **97**, 5007 (1992).

- ¹⁷V. Parasuk and J. Almlöf, Chem. Phys. Lett. **184**, 187 (1991).
- ¹⁸M. Saito and Y. Miyamoto, Phys. Rev. Lett. **87**, 035503 (2001).
- ¹⁹M. Saito and Y. Miyamoto, Phys. Rev. B **65**, 165434 (2002).
- ²⁰T. Yamamoto *et al.*, Phys. Rev. Lett. **95**, 065501 (2005).
- ²¹F. Lin *et al.*, arXiv:0706.0331.
- ²²E. R. Gagliano and C. A. Balseiro, Phys. Rev. Lett. **59**, 2999 (1987).
- ²³S. R. White *et al.*, Phys. Rev. B **40**, 506 (1989).
- ²⁴M. Jarrell and J. E. Gubernatis, Phys. Rep. **269**, 133 (1996).
- ²⁵N. P. Konstantinidis, Phys. Rev. B **72**, 064453 (2005).
- ²⁶For large U/t , the neutral molecule ground-state energy can be fitted to $E_{20}/(t^2/U) = a + b(t/U)^2$, where $a = 4E_H/J - 30$ and E_H is the ground-state energy of the Heisenberg model, obtained by exact diagonalization in Ref. 25, $E_H = -9.72219J$. A fit, using ED results for $U/t=50$ and 100, gives $E_H = -9.72217J$.
- ²⁷S. R. White *et al.*, Phys. Rev. B **45**, 5062 (1992).
- ²⁸S. Chakravarty and S. Kivelson, Europhys. Lett. **16**, 751 (1991).
- ²⁹M. Granath and S. Östlund, Phys. Rev. B **66**, 180501(R) (2002).
- ³⁰F. Lin *et al.*, Phys. Rev. B **71**, 165436 (2005).
- ³¹S. Chakravarty *et al.*, Lett. Math. Phys. **23**, 265 (1991).
- ³²D. Sénéchal *et al.*, Phys. Rev. Lett. **84**, 522 (2000).
- ³³D. Sénéchal *et al.*, Phys. Rev. B **66**, 075129 (2002).